

## Combinatorial Approach To Study Enzyme/Surface Interactions

Katja Loos,<sup>†,‡,§,||</sup> Scott B. Kennedy,<sup>⊥,#</sup> Naomi Eidelman,<sup>⊗</sup> Yian Tai,<sup>○</sup>  
Michael Zharnikov,<sup>○</sup> Eric J. Amis,<sup>⊥</sup> Abraham Ulman,<sup>†,§,▽</sup> and  
Richard A. Gross<sup>\*,†,‡</sup>

*Othmer Department of Chemical and Biological Sciences and Engineering, Polytechnic University, 6 Metrotech Center, Brooklyn, New York 11201; The National Science Foundation Center for Biocatalysis & Bioprocessing of Macromolecules; The National Science Foundation Garcia MRSEC for Polymers at Engineered Interfaces; Polymers Division, National Institute of Standards & Technology, Gaithersburg, Maryland 20899; Paffenbarger Research Center, American Dental Association Foundation, Polymers Division, National Institute of Standards & Technology, Gaithersburg, Maryland 20899; and Angewandte Physikalische Chemie, Universitt Heidelberg, Im Neuenheimer Feld 253, 69120 Heidelberg, Germany*

Received December 14, 2004. In Final Form: March 31, 2005

A fast combinatorial approach to access information about the immobilization behavior and kinetics of enzymes on a variation of surfaces is presented. As a test system, *Candida Antarctica Lipase B* was immobilized on a self-assembled monolayer bearing a gradient of surface energy. The respective immobilization behavior was monitored by Fourier transform infrared microspectroscopy. In addition, the activity of the immobilized enzyme was monitored over the entire film in real time with a specially developed fluorescence activity assay embedded into a siloxane gel. It was found that the highest amount of active protein was immobilized on the hydrophilic end of the gradient surface. This effect is associated with a higher surface roughness of this area resulting in hydrophobic microenvironments in which the enzyme gets immobilized.

### Introduction

Enzymes have excellent features (activity, selectivity, specificity) for designing synthetic processes to obtain a wide range of products under mild and environmentally friendly conditions.<sup>1</sup> However, enzymes have been optimized via natural evolution to fulfill their biological function: catalyzing reactions in complex metabolic pathways exposed to many levels of regulation. Therefore, natural enzymes seldom have the features adequate to be used as industrial catalysts in organic synthesis. The operational conditions of chemical processes are far from the biological environment in which enzymes flourish in nature. Enzymes can denature due to solvent effects and mechanical shear. Recovery of enzymes from reaction solutions and separation of the enzymes from substrates

and products are generally difficult. The productivity (space, time, and yield) of enzymatic processes is often low due to substrate and/or product inhibition.

An important route to improving enzyme performance in non-natural environments is to immobilize them by either adsorption, covalent attachment, or incorporation in hydrophobic organic–inorganic hybrid materials by a sol–gel process.<sup>2</sup> These immobilization procedures have resulted in remarkable improvements in enzyme activity (up to a factor of 100), long-term stability, increased enantioselectivity, and more. The increased stability is due to the fact that enzyme activity will change as a function of its local environment (e.g., solvent polarity, surface chemistry). However, it is important to move beyond general correlations to a better understanding on a molecular level of how immobilization on surfaces can stabilize and activate protein catalysts.

For this purpose, molecularly engineered surfaces are necessary, and one method to produce these can be provided by self-assembled monolayers (SAMs).<sup>3</sup> These systems give a powerful tool to study biological processes on a variety of well-defined substrates. The formation of such monolayer systems is extremely versatile and can provide a method for the in vitro development of biosurfaces that mimic naturally occurring molecular recognition processes.<sup>4</sup>

The most frequently employed enzymes in chemical synthesis, especially for trans-esterifications in organic media, are lipases. Lipases are triacylglycerol hydrolases

\* To whom correspondence should be addressed. E-mail: r.gross@poly.edu.

<sup>†</sup> Polytechnic University.

<sup>‡</sup> The National Science Foundation Center for Biocatalysis & Bioprocessing of Macromolecules.

<sup>§</sup> The National Science Foundation Garcia MRSEC for Polymers at Engineered Interfaces.

<sup>||</sup> Present address: University of Groningen, Polymer Chemistry & Materials Science Center, Nijenborgh 4, 9747 AG Groningen, The Netherlands.

<sup>⊥</sup> Polymers Division, National Institute of Standards & Technology.

<sup>#</sup> Present address: Eastern Mennonite University, Chemistry Department, 1200 Park Road, Harrisonburg, VA 22802.

<sup>⊗</sup> Paffenbarger Research Center, National Institute of Standards & Technology.

<sup>○</sup> Universität Heidelberg.

<sup>▽</sup> Present address: Bar-Ilan University, Department of Chemistry, Ramat Gan 52900, Israel.

(1) (a) Drauz, K., Waldmann, H., Eds. *Enzyme catalysis in organic synthesis: A comprehensive handbook*; Wiley-VCH: Weinheim, 2002; Vol. I. (b) Silverman, R. B. *The Chemistry of Enzyme-Catalyzed Reactions*; Academic Press: San Diego, 2000. (c) Faber, K. *Biotransformations in Organic Chemistry*, 4th ed.; Springer: Berlin, 2000.

(2) (a) Reetz, M. T.; Tielmann, P.; Wiesenhofer, W.; Konen, W.; Zonta, A. *Adv. Synth. Catal.* **2003**, *345*, 717. (b) Dumitriu, E.; Secundo, F.; Patarin, J.; Fechet, L. *J. Mol. Catal. B: Enzym.* **2003**, *22*, 119. (c) Chan, C. M.; Ko, T. M.; Hiraoka, H. *Surf. Sci. Rep.* **1996**, *24*, 3. (d) Goldstein, L. *Methods Enzymol.* **1987**, *135*, 90. (e) Dyal, A.; Loos, K.; Noto, M.; Chang, S.; Spagnoli, C.; Shafi, K.; Ulman, A.; Cowman, M.; Gross, R. *J. Am. Chem. Soc.* **2003**, *125*, 1684.

(3) (a) Ulman, A. *Chem. Rev.* **1996**, *96*, 1533. (b) Ulman, A. *Acc. Chem. Res.* **2001**, *34*, 855.

(EC 3.1.1.3) produced in intra- and extracellular compartments that are responsible for the digestion of lipids in the organism metabolism. They possess a broad range of catalytic activities for chemical synthesis.<sup>5</sup> *Candida antarctica* lipase B (CAL-B) was selected for this investigation of surface interactions because of its extensive use in organic synthesis and polymerizations. Considering that a variety of different surfaces should be probed, which can be time-consuming, we used a novel combinatorial approach to explore, in a single experiment, enzyme interactions with multiple surface chemistries. This approach is based on studies of the immobilization behavior of lipase on surfaces having a gradient in surface energy. Gradient surfaces are well-suited to interrogate the behavior of polymers,<sup>6</sup> proteins,<sup>7</sup> cells,<sup>8</sup> and so forth. Surface gradients were prepared by the gradual exposure of an octadecyltrimethoxysilane (ODTS) SAM on commercial glass slides to UV/O<sub>3</sub>. The surface energy gradient along the glass slide was assessed by contact angle measurements. A fluorescence activity assay based on the lipase-catalyzed transesterification of 6,8-difluoro-4-methylumbelliferyl octanoate (DIFMU octanoate) in acetonitrile to 6,8-difluoro-7-hydroxy-4-methylcoumarin (DIFMU) was developed to assess the enzyme activity on the gradient surface. With this at hand it has become possible to spatially resolve the enzyme kinetic information from different positions along the gradient surface simultaneously and in real time.

### Experimental Section

Acetonitrile (dry), dimethoxydimethylsilane, hexanol (dry), tetramethyl orthosilicate, octadecyl trimethoxysilane (ODTS), toluene (dry), octadecanethiol (ODT) (all Aldrich), DIFMU octanoate (Molecular Probes), and CAL-B (in Tris buffer) (Novozymes) were used without further purification. Water was purified via a Millipore Milli-Q system.

Monolayers of ODTS were produced by submerging the glass slides into a 3 wt % solution of ODTS in toluene overnight. After this, the glass slides were washed at least three times with toluene and then annealed in a vacuum oven at 10 mbar and 120 °C for 24 h. For the activity studies, commercial microscopy glass slides (Fisher Scientific) were utilized, whereas reflective glass slides (2.5 cm × 7.5 cm, Kevley Technologies, Chesterland, OH) were used for the Fourier transform infrared (FTIR) microspectroscopy experiments.

Gradient surfaces were produced by treatment of the monolayer for 5 min with UV/O<sub>3</sub> in a UV/O<sub>3</sub> cleaner (342 UV cleaner, Jelight Co., Inc., Irvine, CA, U.S.A., and UVOCs T0606B ultra-

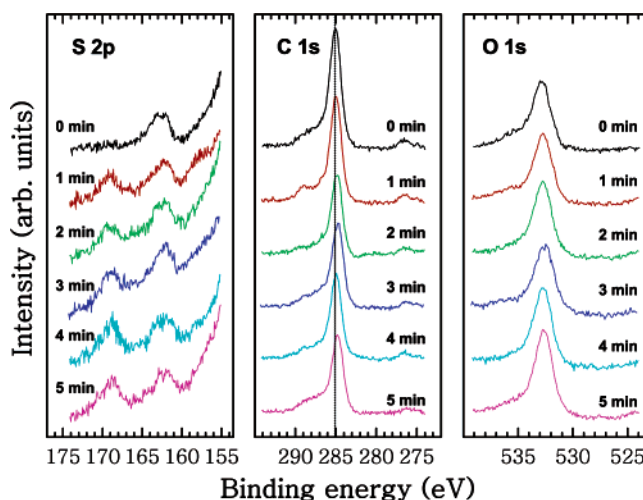


**Figure 1.** S(2p), C(1s), and O(1s) XPS spectra of ODT/Au exposed to UV/O<sub>3</sub> for different time periods.

violet ozone cleaning system, UVOCs, Inc., Montgomeryville, PA) through a fused silica linear variable neutral density filter (Reynard Corp., San Clemente, CA).<sup>9</sup> The process produced a gradient in surface energy along the glass slide that was assessed by contact angle measurements. Static contact angle measurements of water droplets ( $\Theta_{\text{H}_2\text{O}}$ ) were conducted with a Krüss G2 contact angle measuring system (Krüss GmbH, Hamburg, Germany). The results were reproducible, and the gradient spans from 85 to  $45 \pm 5^\circ \Theta_{\text{H}_2\text{O}}$ .

To gain information on the chemistry of the gradient surface we mimicked different spots of the gradient by preparing six homogeneous samples of ODT SAMs on gold and exposing them to UV/O<sub>3</sub>, for 0–5 min. Note that the gold substrates were immersed into a 100  $\mu\text{mol/L}$  solution of ODT in ethanol overnight, subsequently washed three times with the solvent, and dried with a soft stream of nitrogen. The UV/O<sub>3</sub>-induced changes in chemistry were monitored by X-ray photoelectron spectroscopy (XPS). The XPS measurements were performed with a Mg K $\alpha$  X-ray source and an LHS 12 spectrometer in normal emission geometry. The X-ray source was operated at 260-W power and positioned  $\approx 1$  cm away from the samples. The energy resolution was  $\approx 0.9$  eV. The energy scale was referenced to the Au(4f<sub>7/2</sub>) peak at 84.0 eV. For each sample, a wide scan spectrum and the C(1s), O(1s), S(2p), and Au(4f) (not shown) narrow scan spectra were measured. The narrow scan spectra were normalized to the integral intensity of the wide scan spectra to correct for small differences in sample positions and X-ray source intensities.

The immobilization of the enzyme onto the gradient surface was performed by submerging the substrate completely into a 20  $\mu\text{g/mL}$  CAL-B solution in Tris buffer overnight at room temperature. After this, the glass slide was removed from the solution, shaken to remove residual solution, and washed once with 1 mL of water (by letting it run over the slide and shaking nonimmobilized residues away).

Reflective glass slides were used to perform FTIR microspectroscopy measurements on the films. Subjecting the enzyme film coated reflective slides to FTIR microspectroscopy in reflectance mode results in reflection–transmission spectra (FTIR-RTM).<sup>10</sup> These spectra are equivalent to traditional absorption spectra after converting them to absorbance without any mathematical correction.<sup>11</sup> The FTIR-RTM measurements were performed with a Nicolet Magna-IR 550 FTIR spectrophotometer interfaced with a Nic-Plan IR microscope. The microscope is equipped with a video camera, a liquid nitrogen-cooled mercury cadmium telluride detector (Nicolet Instrumentations, Inc., Madison, WI), and a computer-controlled mapping translation stage (Spectra-Tech, Inc., Shelton, CT) which is programmable in the *x* and *y* directions.

(9) Roberson, S.; Fahey, A. J.; Sehgal, A.; Karim, A. *Appl. Surf. Sci.* **2002**, *200*, 150.

(10) Eidelman, N.; Simon, C. G. *J. Res. Natl. Inst. Stand. Technol.* **2004**, *109*, 123.

(11) Rafferty, D. W.; Virnelson, R. C. *Spectroscopy* **1997**, *12*, 42.

(4) (a) Ostuni, E.; Grzybowski, B. A.; Mrksich, M.; Roberts, C. S.; Whitesides, G. M. *Langmuir* **2003**, *19*, 1861. (b) Kada, G.; Riener, C. K.; Hinterdorfer, P.; Kienberger, F.; Stoh, C. M.; Gruber, H. J. *Single Mol.* **2002**, *3*, 119. (c) Petrash, S.; Cregger, T.; Zhao, B.; Pokidysheva, E.; Foster, M. D.; Brittain, W. J.; Sevastianov, V.; Majkrzak, C. F. *Langmuir* **2001**, *17*, 7645. (d) Ostuni, E.; Yan, L.; Whitesides, G. M. *Colloids Surf., B* **1999**, *15*, 3.

(5) (a) Gross, R. A.; Kalra, B.; Kumar, A. *Appl. Microbiol. Biotechnol.* **2001**, *55*, 655. (b) Matsumura, S. *Macromol. Biosci.* **2002**, *2*, 105. (c) Reetz, M. T. *Tetrahedron* **2002**, *58*, 6595. (d) Secundo, F.; Carrea, G. *J. Mol. Catal. B: Enzym.* **2002**, *19*, 93. (e) Uyama, H.; Kobayashi, S. *J. Mol. Catal. B: Enzym.* **2002**, *19*, 117. (f) Krishna, S. H.; Karanth, N. G. *Catal. Rev. Sci. Eng.* **2002**, *44*, 499.

(6) Smith, A. P.; Sehgal, A.; Douglas, J. F.; Karim, A.; Amis, E. J. *Macromol. Rapid Commun.* **2003**, *24*, 131.

(7) (a) Elwing, H.; Welin, S.; Askendal, A.; Nilsson, U.; Lundström, I. *J. Colloid Interface Sci.* **1987**, *119*, 203. (b) Gölander, C.-G.; Lin, Y.-S.; Hlady, V.; Andrade, J. D. *Colloids Surf.* **1990**, *49*, 289. (c) Warkentin, P.; Wälivaara, B.; Lundström, I.; Tengvall, P. *Biomaterials* **1994**, *15*, 786. (d) Spijker, H. T.; Bos, R.; van Oeveren, W.; de Vries, J.; Busscher, H. J. *Colloids Surf., B* **1990**, *15*, 89.

(8) (a) Ruardy, T. G.; Schakenraas, J. M.; van der Mei, H. C.; Busscher, H. J. *Surf. Sci. Rep.* **1997**, *29*, 1. (b) Spijker, H. T.; Busscher, H. J.; van Oeveren, W. *Thromb. Res.* **2003**, *108*, 57. (c) Meredith, J. C.; Sormana, J. L.; Keselowsky, B. G.; Garcia, A. J.; Tona, A.; Karim, A.; Amis, E. J. *J. Biomed. Mater. Res. A* **2003**, *66*, 483. (d) Lee, S. J.; Khang, G.; Lee, Y. M.; Lee, H. B. *J. Colloid Interface Sci.* **2003**, *259*, 228.

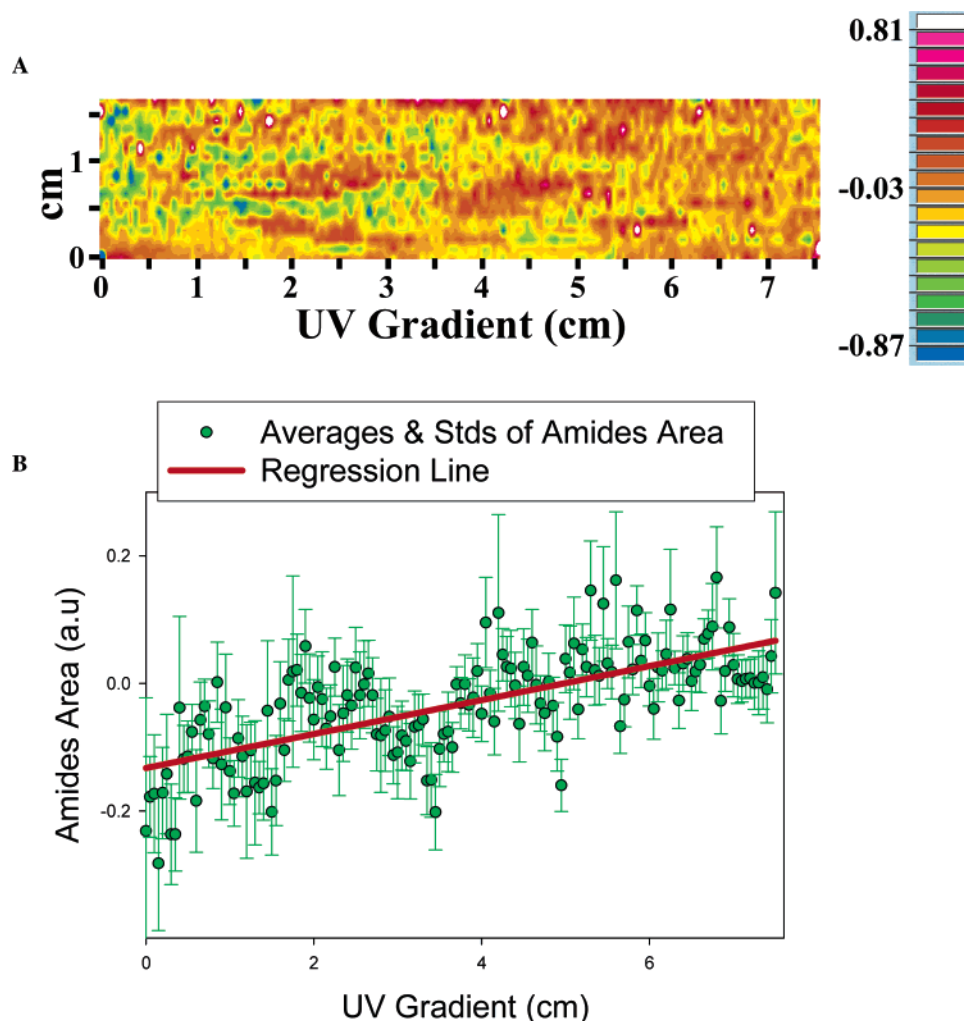


**Figure 2.** (a) FTIR-RTM amides map of CAL-B immobilized on a gradient surface (hydrophobic side to the left, hydrophilic side to the right). A gradient in the areas of the amide peaks is seen from left to right. Blue indicates the lowest amount of amides and red indicates the highest. (b) Averages of the areas of the amide peaks, their standard deviations from the mean, and the linear regression line across the gradient. The error bars refer to one standard deviation of the mean and are taken as an estimate of the uncertainty of the measurement. The trend of increasing amounts of enzyme amides from left to right can be seen.

The spectral point-by-point mapping of the film gradient was done in a grid pattern with a computer-controlled microscope stage and Atlas software package. Spectra were collected from 4000 to 650  $\text{cm}^{-1}$  at a spectral resolution of 8  $\text{cm}^{-1}$  with 32 scans and a beam spot size of 400  $\mu\text{m} \times 400 \mu\text{m}$ . The spectra were normalized to the background of bare spots in the reflective slide. The background was successively measured during the mapping after every 20 spectra to compensate for slight changes in the chamber atmosphere. The resulting images were displayed as color contour maps of the amides in the 1480–1700  $\text{cm}^{-1}$  spectral region. The gradient film was mapped at every 500  $\mu\text{m}$  across the gradient direction ( $x$  axis) and every 1000  $\mu\text{m}$  across the presumed constant  $y$ -axis direction. A total of 3171 spectra were collected in a matrix of 151  $\times$  21 selected points. The gradient map was also imported into the recently revised ISys software<sup>10</sup> (Spectra Dimensions, Olney, MD), and the areas under the amide peaks were obtained for each spectrum of the map. These values were exported from the ISys package, and their averages and standard deviation from the mean perpendicular to the gradient direction were plotted.

To determine the activity of the enzyme on the gradient surface we developed a fluorescence activity assay based on the lipase-catalyzed conversion by transesterification in acetonitrile of DIFMU octanoate to DIFMU that has fluorescence activity. To prevent drying out and mixing by dewetting, we confined the activity assay to a highly viscous matrix. As it is known that lipases show enhanced activity in siloxane gels,<sup>12</sup> we utilized a gel derived from dimethoxydimethylsilane and tetramethyl orthosilicate to confine the assay. This newly developed assay

provided a method by which kinetic information of enzyme activity from different positions along the gradient stripe could be simultaneously collected in real time.

For the fluorescence activity assay 50  $\mu\text{L}$  of a 1 mmol/L solution of DIFMU octanoate in dry acetonitrile was mixed with 50  $\mu\text{L}$  of a 1 mmol/L solution of hexanol in dry acetonitrile and 2900  $\mu\text{L}$  of dry acetonitrile. The 1 mmol/L stock solution of DIFMU octanoate in dry acetonitrile can be stored for about 1 week in the freezer whereas the activity assay starts to develop fluorescent activity by itself about 10–15 h after mixing.

For the gel fluorescence activity assay 2 mL of dimethoxydimethylsilane was thoroughly mixed with 2 mL of tetramethyl orthosilicate. Then, 2 mL of  $\text{H}_2\text{O}$  and 1 mL of the fluorescence activity assay were added and the mixture was shaken until it started to gel. After about 1 h the well-mixed fluorescent activity assay solution has a honeylike consistency. A total of 100  $\mu\text{L}$  of this viscous assay was transferred by an Eppendorf pipet onto selected locations of the gradient surface. The viscous consistency of the solution ensures that it does not further spread on the gradient surface after its transfer.

Fluorescence imaging was conducted on a Bio-Rad VersaDoc 5000 imaging system (Exciter broadband UV, Emitter 450AF58

(12) (a) Reetz, M. T.; Wenkel, R.; Avnir, D. *Synthesis* **2000**, 781. (b) Furukawa, S.-Y.; Kawakami, K. *J. Ferment. Bioeng.* **1998**, *85*, 240. (c) Reetz, M. T. *Adv. Mater.* **1997**, *9*, 943. (d) Reetz, M. T.; Zonta, A.; Simpelkamp, J.; Rufinska, A.; Tesche, B. *J. Sol.-Gel Sci. Technol.* **1996**, *7*, 35. (e) Pierre, M.; Buisson, P.; Fache, F.; Pierre, A. *Biocatal. Biotransform.* **2000**, *18*, 237.

(Omega Optical) equipped with a high-sensitivity charge-coupled device camera (Bio-Rad, Hercules, CA). Measurements were performed using a UV epi-illumination with 2-s single exposures. Images were recorded and quantified with Quantity One software (version 4.40).

Scanning force microscopy images were measured on a Digital Nanoscope (Dimension 3100 Nanoscope IIIa, Veeco Instruments, Inc., Woodbury, NY).

### Results and Discussion

The S(2p), C(1s), and O(1s) XPS spectra of ODT/Au exposed to UV/O<sub>3</sub> for different time periods are presented in Figure 1. The major UV/O<sub>3</sub>-induced changes include a reduction of the S(2p) doublet at  $\approx 162$  eV [S(2p<sub>3/2</sub>)] related to the thiolate headgroups, the appearance of a new S(2p) doublet at  $\approx 168.6$  eV characteristic for sulfonates, a decrease of the C(1s) signal, and an increase of the O(1s) signal. The changes suggest a continuous transformation of the pristine thiolate headgroups into sulfonates and a partial film desorption. In particular, there is a thickness reduction by 18%<sup>13</sup> and oxidation of 46% of the thiolate species after 5 min of the UV/O<sub>3</sub> treatment. In addition, the low binding energy (BE) shift of the main C(1s) emission indicates that cross-links and cleaved bonds are present in the residual film.<sup>8</sup> Furthermore, constancy of the high BE shoulder in the C(1s) spectra related to the C–O and C=O species shows that the oxidation of the alkyl matrix only occurred to a small extent.<sup>14</sup> Note that all observed changes are in good agreement with earlier results on irradiation of SAMs with UV light under ambient conditions.<sup>15</sup> Thus, results of the ODT/Au experiments imply that there was no extended oxidation at the SAM–ambient interface in the course of the UV/O<sub>3</sub> treatment. Instead, an increase in the surface roughness occurs as a consequence of random desorption events. This is also true for the ODTS-based gradient surfaces which was further confirmed by atomic force microscopy (AFM) experiments. The AFM images exhibit an enhanced surface roughness of the SAM, which was moderate on the side with minimum UV/O<sub>3</sub> exposure and more severe on the side with maximum exposure to UV/O<sub>3</sub>. Because surface roughness is known to change the surface energy,<sup>16</sup> we believe that the major factor responsible for changes in the water contact angle along the ODTS-based gradient surface was the corresponding change in surface roughness.

As mentioned above, the enzyme was immobilized overnight from a buffer solution on a gradient surface, and nonimmobilized residues were washed away with water. Figure 2a shows the amide FTIR-RTM map of the gradient surface with physically immobilized CAL-B. The map clearly shows that by this method a gradient thin film of enzyme that overlays the gradient in surface energy was formed. The highest amount of enzyme (red and blue

(13) This is a thickness reduction of the ODT SAM upon a prolonged UV/O<sub>3</sub> exposure. The thickness values were estimated from the analysis of the XPS data assuming a standard exponential attenuation of the XPS signal. For this purpose, the intensities of the Au(4f) ( $I_{Au4f}$ ) and C(1s) ( $I_{C1s}$ ) emissions were evaluated. On the basis of the respective intensity values, the thicknesses of the pristine and UV/O<sub>3</sub>-processed ODS SAMs were determined from the  $I_{C1s}/I_{Au4f}$  and  $I_{C1s}/I_{Ag3d}$  ratios. For the evaluation, the attenuation lengths were used as reported in Lamont, C. L. A.; Wilkes, J. *Langmuir* **1999**, *15*, 2037.

(14) Note that the pristine films were partly oxidized, which was probably related to constraints of the film fabrication procedure.

(15) (a) Vig, J. R. *J. Vac. Sci. Technol., A* **1985**, *3*, 1027. (b) Brunner, H.; Vallant, T.; Mayer, U.; Hoffmann, H. *Langmuir* **1996**, *12*, 4614. (c) Lewis, M.; Tarlov, M. J.; Carron, K. J. *Am. Chem. Soc.* **1995**, *117*, 9574. (d) Hutt, D. A.; Leggett, G. J. *J. Phys. Chem. B* **1996**, *100*, 6657. (e) Hutt, D. A.; Cooper, E.; Leggett, G. J. *J. Phys. Chem. B* **1998**, *102*, 174. (f) Cooper, E.; Leggett, G. J. *Langmuir* **1998**, *14*, 4795. (g) Riely, H.; Kendall, G. K.; Zemical, F. W.; Smith, T. L.; Yang, S. *Langmuir* **1998**, *14*, 5147.

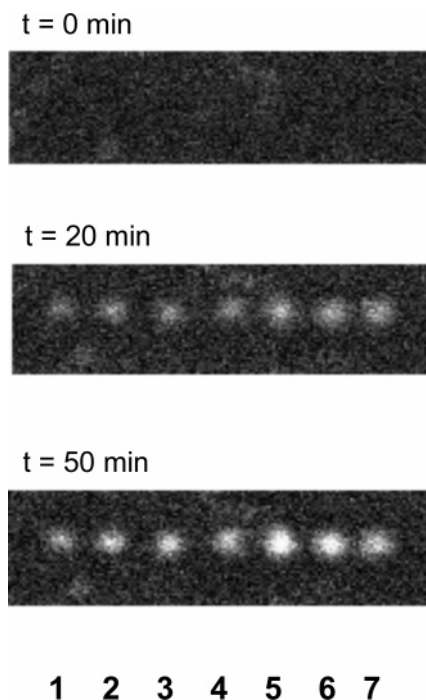


**Figure 3.** Determination of the activity of CAL-B immobilized on a gradient surface (hydrophobic side to the left, hydrophilic side to the right). The lipase-catalyzed transesterification of DIFMU octanoate embedded in a highly viscous siloxane matrix (100- $\mu$ L drops) to DIFMU (fluorescence activity) is monitored by fluorescence imaging.

indicates the highest and lowest amounts of enzyme, respectively) is immobilized on the hydrophilic side of the gradient, even though lipases generally prefer hydrophobic environments. This behavior can again be explained by the irradiation damage of the monolayer. Holes and stripes caused by irradiation-induced desorption of hydrocarbon fragments create cavities that provide desirable hydrophobic microenvironments for the enzyme. The gradient trend shown by FTIR-RTM is in agreement with the other methods used in this study to characterize the enzymes films. Figure 2b shows the averages of the areas of the amide peaks, standard deviation from the mean, and linear regression line across the gradient. A clear trend of increasing amounts of enzyme from left to right was found based on observed intensities of the corresponding enzyme-associated amide vibrational bands. Because the total amounts of the adsorbed enzyme were low across the gradient, the absorbance was quite low, and the atmospheric water that absorbs in the same spectral region interfered in many of the spectra. This might explain the relatively high standard deviations and fluctuations in the trend of adsorbed enzyme. An effort will be made in future adsorption studies to use higher concentrations of enzymes and thereby increase the relative intensity of the amide signal so that the trends of gradients in the FTIR-RTM map are better defined.

Figure 3 shows the images of fluorescence activity along the gradient stripe at different times. Clearly, the highest fluorescent activity develops at the hydrophilic side of the gradient, where the highest amount of enzyme was immobilized. It is even possible to quantify the fluorescence

(16) (a) Chen, Y. L.; Helm, C. A.; Israelachvili, J. N. *J. Phys. Chem.* **1991**, *95*, 10736. (b) Chailapakul, O.; Crooks, R. M. *Langmuir* **1993**, *9*, 884. (c) Guo, L.; Facci, J.; McLendon, G.; Mosher, R. *Langmuir* **1994**, *10*, 4588. (d) Heister, K.; Zharnikov, M.; Grunze, M.; Johansson, L. S. O.; Ulman, A. *Langmuir* **2001**, *17*, 8. (e) Zharnikov, M.; Grunze, M. *J. Vac. Sci. Technol., B* **2002**, *20*, 1793. (f) Gupta, P.; Loos, K.; Kornikow, A.; Spagnoli, C.; Cowman, M.; Ulman, A. *Angew. Chem.* **2004**, *116*, 527.

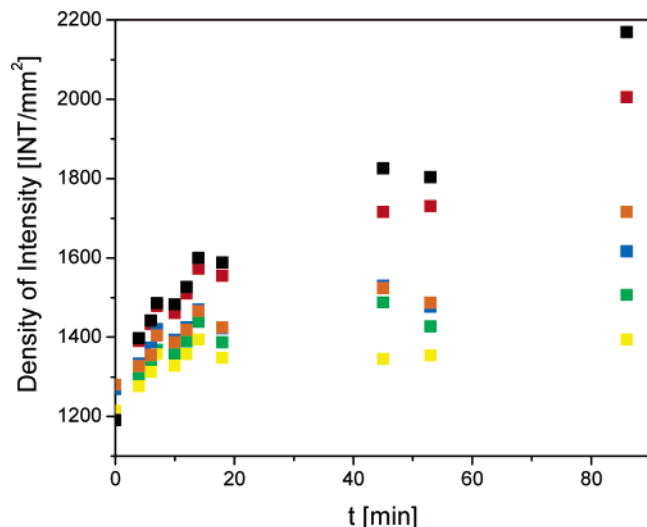


**Figure 4.** Kinetic behavior of the lipase-catalyzed transesterification of DIFMU octanoate embedded in a highly viscous siloxane matrix to DIFMU (fluorescence activity) of CAL-B immobilized on a gradient surface. The density of intensity refers to the discrete points in Figure 3. (yellow) Point 1, (green) point 2, (blue) point 3, (orange) point 4, (red) point 5, and (black) point 6. (Because the fused silica gradient slide that was used to create the surface energy gradient was slightly shorter than the glass slide, point 7 might have been out of the gradient range and, therefore, was excluded).

activity images to obtain kinetic information of CAL-B on the gradient surface. Figure 4 represents the kinetic behavior of CAL-B at the spots shown in Figure 3. The kinetic curves are typical to normal pseudo-first-order kinetics of enzymatic reactions. Not surprisingly, the fastest increase in the fluorescence activity occurred on the hydrophilic side of the gradient, where the highest amount of enzyme was finally immobilized, but without detailed information on the amount of protein immobilized at different locations of the gradient a more quantitative interpretation is not possible.

### Significance and Future Directions

To better characterize the concentration of the protein(s) along gradients, known amounts of adsorbed enzymes will be prepared and measured by FTIR-RTM. This will permit the construction of a calibration curve<sup>10</sup> and determination of the specific activity of the enzyme across the gradient surface. The current and further refined method for creating and characterizing protein gradients can be used as a general tool for many other enzymes and proteins to better understand the complex relationships that govern surface–protein interactions. Important fundamental questions can be addressed in an efficient way, such as how the surface chemistry and topology change the affinity, conformation, and orientation of proteins upon adsorption to surfaces. This can and will be done with advanced microscopy and spectroscopy techniques such as infrared microspectroscopy, circular dichroism reflection, immunofluorescence microscopy, and so forth. Further development of gradient surfaces as a tool to unravel complex relationships between protein–surface interactions and their effect on catalytic activity are currently underway in our laboratories.

Certain commercial materials and equipment are identified for adequate definition of the experimental procedures. In no instance does such identification imply recommendation or endorsement by the ADAF or NIST that the material or the equipment is necessarily the best available for the purpose.

**Acknowledgment.** K.L. is indebted to the Alexander von Humboldt Foundation for financial support. M.Z. and Y.T. thank M. Grunze for support. N.E. thanks the ADAF and NIST for their support. We are grateful to the members of the NSF I/UCRC for Biocatalysis and Bioprocessing of Macromolecules at the Polytechnic University for their financial support, helpful discussions, and encouragement to pursue this research. We also thank Novozymes for providing us with enzymes.

LA0469304